Symplectic discretization for spectral element solution of Maxwell's equations

2009 J. Phys. A: Math. Theor. 42 325203

(http://iopscience.iop.org/1751-8121/42/32/325203)

IOP PUBLISHING JOURNAL OF PHYSICS A: MATHEMATICAL AND THEORETICAL

J. Phys. A: Math. Theor. **42** (2009) 325203 (12pp) doi:10.1088/1751-8113/42/32/325203

Symplectic discretization for spectral element solution of Maxwell's equations

Yanmin Zhao[1,2], Guidong Dai[1,2], Yifa Tang[1] and Qinghuo Liu[3]

[1] LSEC, ICMSEC, Academy of Mathematics and Systems Science, Chinese Academy of Sciences, Beijing 100190, People's Republic of China
[2] Graduate School of the Chinese Academy of Sciences, Beijing 100190, People's Republic of China
[3] Department of Electrical and Computer Engineering, Duke University, Box 90291, Durham, NC 27708, USA

E-mail: tyf@lsec.cc.ac.cn

Received 21 March 2009, in final form 9 June 2009
Published 24 July 2009
Online at stacks.iop.org/JPhysA/42/325203

Abstract

Applying the spectral element method (SEM) based on the Gauss–Lobatto–Legendre (GLL) polynomial to discretize Maxwell's equations, we obtain a Poisson system or a Poisson system with at most a perturbation. For the system, we prove that any symplectic partitioned Runge–Kutta (PRK) method preserves the Poisson structure and its implied symplectic structure. Numerical examples show the high accuracy of SEM and the benefit of conserving energy due to the use of symplectic methods.

PACS numbers: 02.60.Lj, 03.50.De

(Some figures in this article are in colour only in the electronic version)

1. Introduction

Electromagnetic fields have been among the most focused research objects since the age when the classic theory was built, due to their extremely diverse applications in engineering, communication and many other research fields. Maxwell's equations are the fundamental laws describing the motions and behaviors of classic electromagnetic fields, and the starting point for many deliberate and elegant research works. As time-domain simulations were introduced for the analysis of transient electromagnetic fields and sensing systems, numerical solutions of time-domain Maxwell's equations have been more and more common. The finite difference time-domain method (FDTDM) [1] is the original numerical method for Maxwell's equations and turns out to be the most popular tool. Then, various time-domain finite element methods (TDFEM) [2]–[11], including the time-domain spectral element method (SEM) based on Gauss–Lobatto–Legendre (GLL) polynomials [9]–[11], are developed to solve

Maxwell's equations because of their geometric flexibility. The time-domain GLL-SEM has the advantages of high accuracy and geometric flexibility. On account of the orthogonality of the basis functions, a diagonal or a block-diagonal mass matrix can be obtained by using the GLL quadrature with little cost. In section 2, our spatial discretization for Maxwell's equations by using the GLL-SEM yields a system of ordinary differential equations, which is a Poisson system or a Poisson system with a perturbation.

Maxwell's equations can be written as an infinite-dimensional Hamiltonian system [12]. Thus, the solution can be recognized as a Hamiltonian flow in a functional space, which preserves the symplectic structure in temporal direction. Symplectic methods [13]–[19] preserve exactly the inherent canonical properties of the continuous Hamiltonian flow. The most popular processes to deal with an infinite-dimensional Hamiltonian system are first dimension reducing which aims to reach a finite-dimensional Hamiltonian system [16], and then symplectic methods constructing. For Maxwell's equations, we want to get a finite-dimensional Hamiltonian system by using SEM, however there exists an inevitable difficulty owing to the non-consistency between the numbers of edges and faces arising from discretizing electric and magnetic fields, respectively. In fact, the obtained ODEs can be cast into a general Poisson system or a Poisson system with a perturbation rather than a desired finite-dimensional Hamiltonian system. Fortunately, the symplectic partitioned Runge–Kutta (PRK) methods will be proved to preserve exactly the Poisson structure and the implied symplectic structure in section 3. And, our numerical experiments will show the superiorities of this kind of symplectic methods over the non-symplectic ones in the sense of conservation of invariants, especially for longtime simulations, and also, the high efficiency and the spectral accuracy of SEM in section 4.

2. Maxwell's equations and spatial discretization

If the medium is isotropic and linear, then Maxwell's equations are written as

$$\begin{cases} \epsilon \dfrac{\partial \mathbf{E}}{\partial t} = \nabla \times \mathbf{H} - \mathbf{J}_s \\ \mu \dfrac{\partial \mathbf{H}}{\partial t} = -\nabla \times \mathbf{E}, \end{cases} \tag{1}$$

where ϵ and μ are the permittivity and the permeability of the medium respectively (they are assumed to be constant for each medium in this paper), E is the electric field intensity, H is the magnetic field intensity, and J_s is the vector electric current density function. If there are only finite kinds of media in the spatial domain Ω, then (1) can be rewritten as a Hamiltonian system

$$\begin{cases} \dfrac{\partial \mathbf{E}}{\partial t} = \dfrac{1}{\epsilon}\nabla \times \mathbf{H} - \dfrac{1}{\epsilon}\mathbf{J}_s = \dfrac{\delta \mathbb{H}}{\delta \mathbf{H}} \\ \dfrac{\partial \mathbf{H}}{\partial t} = -\dfrac{1}{\mu}\nabla \times \mathbf{E} = -\dfrac{\delta \mathbb{H}}{\delta \mathbf{E}} \end{cases} \tag{2}$$

with Hamiltonian functional

$$\mathbb{H}[\mathbf{E}, \mathbf{H}] = \int_\Omega \left[\frac{1}{2\mu}\mathbf{E} \cdot (\nabla \times \mathbf{E}) + \frac{1}{2\epsilon}\mathbf{H} \cdot (\nabla \times \mathbf{H}) - \frac{1}{\epsilon}\mathbf{H} \cdot \mathbf{J}_s \right] \mathrm{d}\Omega.$$

The Hilbert spaces $H_0(\mathrm{curl}, \Omega)$ and $H_0(\mathrm{div}, \Omega)$ are defined as

$$H_0(\mathrm{curl}, \Omega) = \{\mathbf{u} \in (L^2(\Omega))^3; \nabla \times \mathbf{u} \in (L^2(\Omega))^3, \mathbf{n} \times \mathbf{u} \mid_{\partial\Omega} = 0\},$$

$$H_0(\mathrm{div}, \Omega) = \{\mathbf{u} \in (L^2(\Omega))^3; \nabla \cdot \mathbf{u} \in L^2(\Omega), \mathbf{n} \cdot \mathbf{u} \mid_{\partial\Omega} = 0\}.$$

Let $\Omega \subset \mathbb{R}^3$ be a convex polygonal domain, and $\langle \mathbf{U}, \mathbf{V} \rangle = \int_\Omega \mathbf{U} \cdot \mathbf{V} \, \mathrm{d}\Omega$ for any vectors $\mathbf{U}, \mathbf{V} \in \mathbb{R}^3$. Then the weak form of system (2) is to find $\mathbf{E} \in H_0(\mathrm{curl}, \Omega)$, $\mathbf{H} \in H_0(\mathrm{div}, \Omega)$ for all of $\mathbf{E}^* \in H_0(\mathrm{curl}, \Omega)$, $\mathbf{H}^* \in H_0(\mathrm{div}, \Omega)$ such that

$$\begin{cases} \dfrac{\partial}{\partial t} \langle \epsilon \mathbf{E}, \mathbf{E}^* \rangle = \langle \nabla \times \mathbf{H} - \mathbf{J}_s, \mathbf{E}^* \rangle \\ \dfrac{\partial}{\partial t} \langle \mu \mathbf{H}, \mathbf{H}^* \rangle = -\langle \nabla \times \mathbf{E}, \mathbf{H}^* \rangle. \end{cases} \tag{3}$$

We define the spaces of vector basis functions for electric field $\mathbf{E}$ and magnetic field $\mathbf{H}$ on a physical element K, respectively:

$$U_h = \mathrm{span}\{\boldsymbol{\Phi}_1, \ldots, \boldsymbol{\Phi}_{N_e}\}, \qquad V_h = \mathrm{span}\{\boldsymbol{\Psi}_1, \ldots, \boldsymbol{\Psi}_{N_h}\},$$

where N_e and N_h are the numbers of unknowns for the electric and magnetic fields, respectively.

The discrete problem for (3) is to find $\mathbf{E}_h \in U_h$, $\mathbf{H}_h \in V_h$, for all of $\boldsymbol{\Phi}_i \in U_h$ and $\boldsymbol{\Psi}_j \in V_h$, such that

$$\begin{cases} \dfrac{\partial}{\partial t} \displaystyle\sum_{K \in \Gamma_h} \langle \varepsilon \mathbf{E}_h, \boldsymbol{\Phi}_i \rangle_K = \sum_{K \in \Gamma_h} \langle \nabla \times \mathbf{H}_h - \mathbf{J}_s, \boldsymbol{\Phi}_i \rangle_K \\ \dfrac{\partial}{\partial t} \displaystyle\sum_{K \in \Gamma_h} \langle \mu \mathbf{H}_h, \boldsymbol{\Psi}_j \rangle_K = -\sum_{K \in \Gamma_h} \langle \nabla \times \mathbf{E}_h, \boldsymbol{\Psi}_j \rangle_K, \end{cases} \tag{4}$$

where $\bar{\Omega} = \bigcup_{K \in \Gamma_h}$ is a decomposition of $\bar{\Omega}$ and $\{\Gamma_h\}$ is a regular subdivision sequence of Ω.

$\mathbf{E}_h$ and $\mathbf{H}_h$ can be expressed by the basis functions on K:

$$\mathbf{E}_h(\mathbf{X}, t) = \sum_{i=1}^{N_e} e_i^{(K)}(t) \boldsymbol{\Phi}_i(\mathbf{X}), \qquad \mathbf{H}_h(\mathbf{X}, t) = \sum_{j=1}^{N_h} h_j^{(K)}(t) \boldsymbol{\Psi}_j(\mathbf{X}). \tag{5}$$

Substituting (5) into (4), we gain the matrix form of (4):

$$\begin{cases} A \dfrac{\mathrm{d}e(t)}{\mathrm{d}t} = Sh(t) - f(t) \\ B \dfrac{\mathrm{d}h(t)}{\mathrm{d}t} = -S^T e(t), \end{cases} \tag{6}$$

where A, B, S, f, e, h consist of their corresponding elemental matrices or vectors $A^{(K)}, B^{(K)}, S^{(K)}, f^{(K)}, e^{(K)}, h^{(K)}$ respectively, as follows:

$$(f^{(K)})_i = \int_\Omega \mathbf{J}_s^T \boldsymbol{\Phi}_i \, \mathrm{d}x \, \mathrm{d}y \, \mathrm{d}z; \qquad (A^{(K)})_{ij} = \varepsilon \int_\Omega \boldsymbol{\Phi}_i^T \boldsymbol{\Phi}_j \, \mathrm{d}x \, \mathrm{d}y \, \mathrm{d}z;$$

$$(B^{(K)})_{ij} = \mu \int_\Omega \boldsymbol{\Psi}_i^T \boldsymbol{\Psi}_j \, \mathrm{d}x \, \mathrm{d}y \, \mathrm{d}z; \qquad (S^{(K)})_{ij} = \int_\Omega \boldsymbol{\Phi}_i^T (\nabla \times \boldsymbol{\Psi}_j) \, \mathrm{d}x \, \mathrm{d}y \, \mathrm{d}z.$$

When $\mathbf{J}_s = 0$, (6) yields a Poisson system

$$\begin{cases} A \dfrac{\mathrm{d}e(t)}{\mathrm{d}t} = Sh(t) = S \nabla_h \hat{H}(e, h) \\ B \dfrac{\mathrm{d}h(t)}{\mathrm{d}t} = -S^T e(t) = -S^T \nabla_e \hat{H}(e, h), \end{cases} \tag{7}$$

where $\hat{H}(e, h) = \frac{1}{2}(|e|^2 + |h|^2)$. If $\mathbf{J}_s \neq 0$, then (6) turns to be a Poisson system with some perturbation.

3. Symplectic discretization for the Poisson system

Equations (7) is a particular case of the following Poisson system

$$\frac{\mathrm{d}Z}{\mathrm{d}t} = B(Z)\nabla H(Z), \qquad Z = [q_1, \ldots, q_{m_1}; p_1, \ldots, p_{m_2}]^\top \in \mathbb{R}^m, \tag{8}$$

where $m_1 + m_2 = m$, $B(Z) = \begin{bmatrix} O_{m_1} & M \\ -M^\top & O_{m_2} \end{bmatrix}$, $O_{m_i} \in \mathbb{R}^{m_i \times m_i}$ is a null matrix ($i = 1, 2$), $M \in \mathbb{R}^{m_1 \times m_2}$, ∇ stands for the gradient operator, and $H : \mathbb{R}^{m_1+m_2} \to \mathbb{R}^1$ is a smooth function (*Hamiltonian function*).

Let $\mathrm{rank}(M) = r \leqslant \min\{m_1, m_2\}$. Without loss of generality, the $(r \times r)$-sub-matrix on the top-left corner of M is assumed to be non-degenerate. In this context, one can write

$$M = \begin{bmatrix} K \\ CK \end{bmatrix} = \begin{bmatrix} \hat{K} & \hat{K}\hat{C} \\ C\hat{K} & C\hat{K}\hat{C} \end{bmatrix} = \left[V, V\hat{C}\right], \tag{9}$$

where $K \in \mathbb{R}^{r \times m_2}$, $C \in \mathbb{R}^{(m_1-r)\times r}$, $\hat{K} \in \mathbb{R}^{r\times r}$ is non-degenerate, $\hat{C} \in \mathbb{R}^{r\times(m_2-r)}$, and $V \in \mathbb{R}^{m_1\times r}$.

Later, we prove that the Poisson system (8) implies a symplectic structure.

Let $q = [q_1, \ldots, q_r; q_{r+1}, \ldots, q_{m_1}]^\top = [\bar{q}^\top, \hat{q}^\top]^\top$, $p = [p_1, \ldots, p_r; p_{r+1}, \ldots, p_{m_2}]^\top = [\bar{p}^\top, \hat{p}^\top]^\top$, $\bar{q}, \bar{p} \in \mathbb{R}^r$, $\hat{q} \in \mathbb{R}^{m_1-r}$, $\hat{p} \in \mathbb{R}^{m_2-r}$. According to (9), system (8) can be rewritten as

$$\begin{aligned} \frac{\mathrm{d}\bar{q}}{\mathrm{d}t} &= K\nabla_p H\,(q, p)\,, & \frac{\mathrm{d}\bar{p}}{\mathrm{d}t} &= -V^\top \nabla_q H\,(q, p)\,, \\ \frac{\mathrm{d}\hat{q}}{\mathrm{d}t} &= CK\nabla_p H\,(q, p)\,, & \frac{\mathrm{d}\hat{p}}{\mathrm{d}t} &= -\hat{C}^\top V^\top \nabla_q H\,(q, p)\,. \end{aligned} \tag{10}$$

Given initial conditions: $q(0) = q_0 = \left[\bar{q}_0^\top, \hat{q}_0^\top\right]^\top$, $p(0) = p_0 = \left[\bar{p}_0^\top, \hat{p}_0^\top\right]^\top$, (10) brings in $\hat{q} = C\bar{q} + (\hat{q}_0 - C\bar{q}_0)$ and $\hat{p} = \hat{C}^\top\bar{p} + (\hat{p}_0 - \hat{C}^\top\bar{p}_0)$. Let

$$\begin{aligned} \bar{H}\,(\bar{q}, \bar{p}) &= H\,(q, p)\,|_{\hat{q}=C\bar{q}+(\hat{q}_0-C\bar{q}_0),\quad \hat{p}=\hat{C}^\top\bar{p}+(\hat{p}_0-\hat{C}^\top\bar{p}_0)} \\ &= H(\bar{q}, C\bar{q} + (\hat{q}_0 - C\bar{q}_0)\,;\, \bar{p}, \hat{C}^\top\bar{p} + (\hat{p}_0 - \hat{C}^\top\bar{p}_0)), \end{aligned}$$

then

$$\nabla_{\bar{q}}\bar{H} = \nabla_{\bar{q}}H + C^\top\nabla_{\hat{q}}H, \qquad \nabla_{\bar{p}}\bar{H} = \nabla_{\bar{p}}H + \hat{C}\nabla_{\hat{p}}H. \tag{11}$$

According to (9), (11), the first two equations in (10) can be rewritten as

$$\frac{\mathrm{d}\bar{q}}{\mathrm{d}t} = \hat{K}\nabla_{\bar{p}}\bar{H}\,(\bar{q}, \bar{p})\,, \qquad \frac{\mathrm{d}\bar{p}}{\mathrm{d}t} = -\hat{K}^\top\nabla_{\bar{q}}\bar{H}\,(\bar{q}, \bar{p})\,.$$

Thus, we have the following theorem.

Theorem 1. *System (8) can be divided into two parts: one is a Hamiltonian system equivalent to*

$$\begin{cases} \dfrac{\mathrm{d}\bar{q}}{\mathrm{d}t} = \hat{K}\nabla_{\bar{p}}\bar{H}\,(\bar{q}, \bar{p}) \\ \dfrac{\mathrm{d}\bar{p}}{\mathrm{d}t} = -\hat{K}^\top\nabla_{\bar{q}}\bar{H}\,(\bar{q}, \bar{p}) \end{cases} \tag{12}$$

with symplectic structure $\mathrm{d}\bar{p} \wedge \hat{K}^{-1}\,\mathrm{d}\bar{q}$*, the other is a simple algebraic system*

$$\begin{cases} \hat{\mathrm{q}} = C\bar{\mathrm{q}} + (\hat{\mathrm{q}}_0 - C\bar{\mathrm{q}}_0) \\ \hat{\mathrm{p}} = \hat{C}^\top\bar{\mathrm{p}} + (\hat{\mathrm{p}}_0 - \hat{C}^\top\bar{\mathrm{p}}_0). \end{cases} \tag{13}$$

Table 1. Table of Butcher for the PRK method.

c_1	a_{11}	...	a_{1s}	$\bar{c}_1$	$\bar{a}_{11}$	⋯	$\bar{a}_{1s}$
⋮	⋮	⋱	⋮	⋮	⋮	⋱	⋮
c_s	a_{s1}	...	a_{ss}	$\bar{c}_s$	$\bar{a}_{s1}$	⋯	$\bar{a}_{ss}$
	b_1	...	b_s		$\bar{b}_1$	⋯	$\bar{b}_s$

In order to preserve its symplectic structure and the total energy of the system, the symplectic method is the best choice to solve (12). As is well known, the phase flow of any Poisson system is a one-parameter group of Poisson transformations, therefore the structure-preserving algorithms (Poisson schemes) are desirable to be employed to solve this kind of systems. It has been shown that any symplectic implicit diagonal Runge–Kutta method is a Poisson scheme [15]. We will show that actually, for the linear Poisson system (8) (i.e., $B(z)$ is a constant matrix), any symplectic partitioned Runge–Kutta method preserves the Poisson structure and the implied symplectic structure.

Recall that an s-order PRK method given in table 1 is usually used to solve the ordinary differential equations

$$\begin{cases} \dfrac{\mathrm{d}q}{\mathrm{d}t} = f(q, p) \\ \dfrac{\mathrm{d}p}{\mathrm{d}t} = g(q, p). \end{cases} \tag{14}$$

The result is

$$\begin{cases} Q_i = q_0 + h \displaystyle\sum_{j=0}^{s} a_{ij} f(Q_j, P_j) \\ P_i = p_0 + h \displaystyle\sum_{j=0}^{s} \bar{a}_{ij} g(Q_j, P_j) \\ q_1 = q_0 + h \displaystyle\sum_{j=0}^{s} b_j f(Q_j, P_j) \\ p_1 = p_0 + h \displaystyle\sum_{j=0}^{s} \bar{b}_j g(Q_j, P_j). \end{cases}$$

The symplectic condition of this PRK method is [14]

$$\begin{cases} b_i \bar{a}_{ij} + \bar{b}_j a_{ji} - b_i \bar{b}_j = 0, & 1 \leqslant i \leqslant s \\ b_i = \bar{b}_i, & 1 \leqslant i \leqslant s. \end{cases} \tag{15}$$

If (12) is a separable system, then the symplectic condition will be reduced to the first formula of (15) only.

Next we introduce a definition and some theorems to analyze the numerical solutions of (8).

Definition 1. *The variables $\bar{q}$, $\bar{p}$ in the Hamiltonian system (12) are called the symplectic components of q and p, respectively; and the variables $\hat{q}$, $\hat{p}$ in the algebraic system (13) are called their non-symplectic components.*

Theorem 2. *Let u denote the numerical solution of the PRK method for (8), then the symplectic components of u are numerical solutions of the PRK method for (12) and the non-symplectic components of u are numerical solutions of the PRK method for (13).*

Proof. Let $(q_0, p_0), (q_1, p_1), \ldots, (q_N, p_N)$ be the numerical solution of sth order PRK method according to table 1 for (8), then

$$\begin{cases} Q_i^n = q_n + h\sum_{j=1}^{s} a_{ij} M\nabla_p H\big(Q_j^n, P_j^n\big) \\ P_i^n = p_n - h\sum_{j=1}^{s} \bar{a}_{ij} M^T \nabla_q H\big(Q_j^n, P_j^n\big) \\ q_{n+1} = q_n + h\sum_{j=1}^{s} b_j M\nabla_p H\big(Q_j^n, P_j^n\big) \\ p_{n+1} = p_n - h\sum_{j=1}^{s} \bar{b}_j M^T \nabla_q H\big(Q_j^n, P_j^n\big) \end{cases}, \quad \begin{array}{l} i = 1, 2, \ldots, s, \\ n = 0, 1, \ldots, N-1. \end{array} \tag{16}$$

Considering $M = \left[\begin{smallmatrix} \hat{K} & \hat{K}\hat{C} \\ C\hat{K} & C\hat{K}\hat{C} \end{smallmatrix}\right]$, from$q_{n+1} = q_n + h\sum_{j=1}^{s} b_j M\nabla_p H\big(Q_j^n, P_j^n\big)$, we obtain

$$\hat{q}_{n+1} = C\bar{q}_{n+1} + (\hat{q}_n - C\bar{q}_n), \qquad n = 0, 1, \ldots, N-1. \tag{17}$$

Recursively, we have

$$\hat{q}_n = C\bar{q}_n + (\hat{q}_0 - C\bar{q}_0), \qquad n = 1, 2, \ldots, N. \tag{18}$$

For $i = 1, 2, \ldots, s;\quad n = 0, 1, \ldots, N-1$, we obtain

$$\hat{Q}_i^n - \hat{q}_n = C\big(\bar{Q}_i^n - \bar{q_n}\big). \tag{19}$$

Based on (18), we have

$$\hat{Q}_i^n = C\bar{Q}_i^n + (\hat{q}_0 - C\bar{q}_0). \tag{20}$$

By using (20) and the definition of $\bar{H}(\bar{q}, \bar{p})$, we obtain

$$\bar{H}\big(\bar{Q}_j^n, \bar{P}_j^n\big) = H\big(Q_j^n, P_j^n\big)\big|_{\hat{Q}_j^n = C\bar{Q}_j^n + (\hat{q}_0 - C\bar{q}_0),\, \hat{P}_j^n = C\bar{P}_j^n + (\hat{p}_0 - \hat{C}^T\bar{p}_0)},$$

then, we derive the following scheme

$$\begin{cases} \bar{Q}_i^n = \bar{q}_n + h\sum_{j=1}^{s} a_{ij}\hat{K}\nabla_{\bar{p}}\bar{H}\big(\bar{Q}_j^n, \bar{P}_j^n\big) \\ \bar{P}_i^n = \bar{p}_n - h\sum_{j=1}^{s} \bar{a}_{ij}\hat{K}^T\nabla_{\bar{q}}\bar{H}\big(\bar{Q}_j^n, \bar{P}_j^n\big) \\ \bar{q}_{n+1} = \bar{q}_n + h\sum_{j=1}^{s} b_j\hat{K}\nabla_{\bar{p}}\bar{H}\big(\bar{Q}_j^n, \bar{P}_j^n\big) \\ \bar{p}_{n+1} = \bar{p}_n - h\sum_{j=1}^{s} \bar{b}_j\hat{K}^T\nabla_{\bar{q}}\bar{H}\big(\bar{Q}_j^n, \bar{P}_j^n\big) \\ \hat{q}_{n+1} = C\bar{q}_{n+1} + (\hat{q}_0 - C\bar{q}_0) \\ \hat{p}_{n+1} = \hat{C}^T\bar{p}_{n+1} + (\hat{p}_0 - \hat{C}^T\bar{p}_0). \end{cases} \tag{21}$$

Equation (21) can be divided into two parts, one is the PRK discretization of (12), and the

other is

$$\begin{cases} \hat{q}_n = C\bar{q}_n + (\hat{q}_0 - C\bar{q}_0) \\ \hat{p}_n = \hat{C}^T\bar{p}_n + (\hat{p}_0 - \hat{C}^T\bar{p}_0). \end{cases} \tag{22}$$

Obviously, (22) is the PRK discretization form of (13). □

Let $L = \begin{bmatrix} O_r & \hat{K} \\ -\hat{K}^T & O_r \end{bmatrix}^{-1}$ ($O_r \in \mathbb{R}^{r\times r}$ is a null matrix), we have the following theorem:

Theorem 3. *Any symplectic PRK method is an L-symplectic scheme for the Hamiltonian system (12), and corresponds to a Poisson integrator for the Poisson system (8).*

4. Numerical results

From Maxwell's equations (1) to Poisson system (7), the spatial discretization is implemented by using the spectral elements based on GLL polynomials.

In the 1D case, on reference element $[-1, 1]$, N th GLL basis functions are defined as

$$\phi_j(\xi) = -\frac{1}{N(N+1)L_N(\xi_j)}\frac{(1-\xi^2)L'_N(\xi)}{\xi - \xi_j}, \qquad j = 0, 1, \ldots N, \tag{23}$$

where $L_N(\xi)$ is Nth Legendre polynomial and ξ_j $(0 \leqslant j \leqslant N)$ are the zero points of $(1-\xi^2)L'_N(\xi)$. Thus, for any polynomial $P(x)$ with degree not higher than $2N-1$, we have $\int_{-1}^{1} P(\xi)\mathrm{d}\xi = \sum_{k=0}^{N}\omega_k P(\xi_k)$, where $\omega_k = \frac{2}{N(N+1)[L_N(\xi_k)]^2}$.

In the 3D case, on the reference element $[-1, 1]\times[-1, 1]\times[-1, 1]$, the basis functions $\mathbf{\Phi}_i = \mathbf{\Phi}_{rst} \in U_h$ can be chosen as

$$\begin{aligned} \mathbf{\Phi}^{\xi}_{rst}(\xi,\eta,\zeta) &= \hat{\xi}\phi_r^{(N_\xi-1)}(\xi)\phi_s^{(N_\eta)}(\eta)\phi_t^{(N_\zeta)}(\zeta); \\ \mathbf{\Phi}^{\eta}_{rst}(\xi,\eta,\zeta) &= \hat{\eta}\phi_r^{(N_\xi)}(\xi)\phi_s^{(N_\eta-1)}(\eta)\phi_t^{(N_\zeta)}(\zeta); \\ \mathbf{\Phi}^{\zeta}_{rst}(\xi,\eta,\zeta) &= \hat{\zeta}\phi_r^{(N_\xi)}(\xi)\phi_s^{(N_\eta)}(\eta)\phi_t^{(N_\zeta-1)}(\zeta); \end{aligned}$$

and the basis functions $\mathbf{\Psi}_i = \mathbf{\Psi}_{rst} \in V_h$ can be chosen as

$$\begin{aligned} \mathbf{\Psi}^{\xi}_{rst}(\xi,\eta,\zeta) &= \hat{\xi}\phi_r^{(N_\xi)}(\xi)\phi_s^{(N_\eta-1)}(\eta)\phi_t^{(N_\zeta-1)}(\zeta); \\ \mathbf{\Psi}^{\eta}_{rst}(\xi,\eta,\zeta) &= \hat{\eta}\phi_r^{(N_\xi-1)}(\xi)\phi_s^{(N_\eta)}(\eta)\phi_t^{(N_\zeta-1)}(\zeta); \\ \mathbf{\Psi}^{\zeta}_{rst}(\xi,\eta,\zeta) &= \hat{\zeta}\phi_r^{(N_\xi-1)}(\xi)\phi_s^{(N_\eta-1)}(\eta)\phi_t^{(N_\zeta)}(\zeta), \end{aligned}$$

where N_ξ, N_η N_ζ are the degrees of GLL basis functions in terms of ξ, η and ζ, respectively.

We choose the above mixed-order curl conforming vector basis functions to guarantee Gauss's law at discrete level [20] and the tangential continuity across the element edges as well as the element surfaces.

Making the best use of the properties of the basis functions for spectral elements [11], one obtains a diagonal mass matrix. For example,

$$\begin{aligned} B^{(1)}_{ij} &= \int_{-1}^{1}\int_{-1}^{1}\int_{-1}^{1}\phi_r^{(N_\xi-1)}(\xi)\phi_s^{(N_\eta)}(\eta)\phi_t^{(N_\zeta)}(\zeta) \\ &\quad\times \phi_{r'}^{(N_\xi-1)}(\xi)\phi_{s'}^{(N_\eta)}(\eta)\phi_{t'}^{(N_\zeta)}(\zeta)\,\mathrm{d}\xi\,\mathrm{d}\eta\,\mathrm{d}\zeta \\ &= \sum_{m=0}^{N_\xi}\sum_{n=0}^{N_\eta+1}\sum_{p=0}^{N_\zeta+1}\omega_m^{(N_\xi)}\omega_n^{(N_\eta+1)}\omega_p^{(N_\zeta+1)} \\ &\quad\times \phi_r^{(N_\xi-1)}(\xi_m)\phi_{r'}^{(N_\xi-1)}(\xi_m)\phi_s^{(N_\eta)}(\eta_n)\phi_{s'}^{(N_\eta)}(\eta_n)\phi_t^{(N_\zeta)}(\zeta_p)\phi_{t'}^{(N_\zeta)}(\zeta_p) \end{aligned}$$

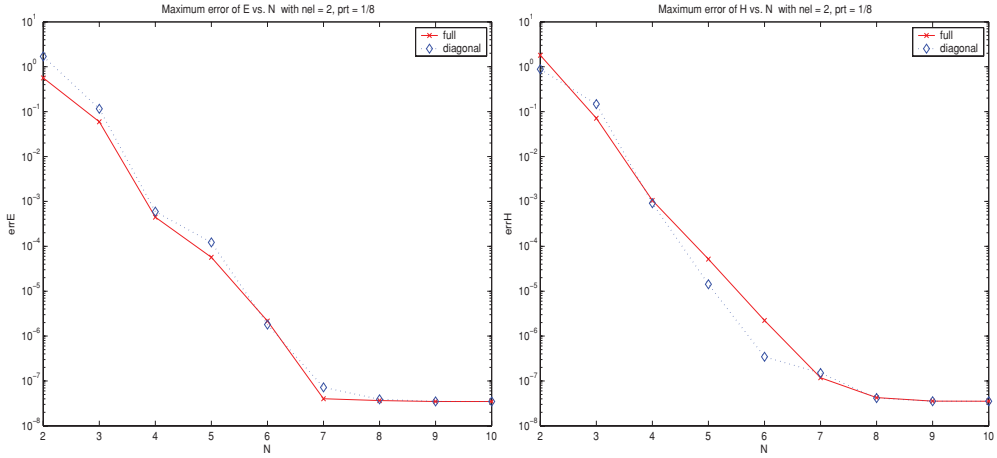

Figure 1. Errors of electric field at 102.125 T obtained by using full and diagonal mass matrices (left); errors of magnetic field at 102.125 T obtained by using full and diagonal mass matrices (right).

Table 2. Table of Butcher for the fourth-order symplectic PRK method.

$\frac{\gamma_1}{2}$	$\frac{\gamma_1}{2}$	0	0	0
$\frac{1}{2}$	$\frac{\gamma_1}{2}$	$\frac{\gamma_1+\gamma_2}{2}$	0	0
$\frac{3\gamma_1+2\gamma_2}{2}$	$\frac{\gamma_1}{2}$	$\frac{\gamma_1+\gamma_2}{2}$	$\frac{\gamma_1+\gamma_2}{2}$	0
1	$\frac{\gamma_1}{2}$	$\frac{\gamma_1}{2}$	$\frac{\gamma_1+\gamma_2}{2}$	$\frac{\gamma_1}{2}$
	$\frac{\gamma_1}{2}$	$\frac{\gamma_1}{2}$	$\frac{\gamma_1}{2}$	$\frac{\gamma_1}{2}$

0	0	0	0	0
γ_1	γ_1	0	0	0
$\gamma_1+\gamma_2$	γ_1	γ_2	0	0
1	γ_1	γ_2	γ_1	0
	γ_1	γ_2	γ_1	0

Table 3. Table of Butcher for the fourth-order non-symplectic RK method.

0	0	0	0	0
$\frac{1}{2}$	$\frac{1}{2}$	0	0	0
$\frac{1}{2}$	0	$\frac{1}{2}$	0	0
1	0	0	1	0
	$\frac{1}{6}$	$\frac{1}{3}$	$\frac{1}{3}$	$\frac{1}{6}$

$$
\begin{aligned}
&\approx \sum_{m=0}^{N_\xi-1}\sum_{n=0}^{N_\eta}\sum_{p=0}^{N_\zeta} \omega_m^{(N_\xi-1)}\omega_n^{(N_\eta)}\omega_p^{(N_\zeta)} \\
&\quad\times \phi_r^{(N_\xi-1)}(\xi_m)\phi_{r'}^{(N_\xi-1)}(\xi_m)\phi_s^{(N_\eta)}(\eta_n)\phi_{s'}^{(N_\eta)}(\eta_n)\phi_t^{(N_\zeta)}(\zeta_p)\phi_{t'}^{(N_\zeta)}(\zeta_p) \\
&= \delta_{rr'}\delta_{ss'}\delta_{tt'}\omega_r^{(N_\xi-1)}\omega_s^{(N_\eta)}\omega_t^{(N_\zeta)}.
\end{aligned}
$$

Exact integration of $B_{ij}^{(1)}$ produces a full mass matrix, whereas the above approximations lead to a diagonal mass matrix which requires much less cost. In the numerical experiments, we will show the errors between the electromagnetic fields obtained by using the full and the diagonal mass matrices.

For 1D and 2D cases, based on the GLL-spectral-element spatial discretization, we will compare the numerical results obtained by using the fourth-order explicit symplectic PRK

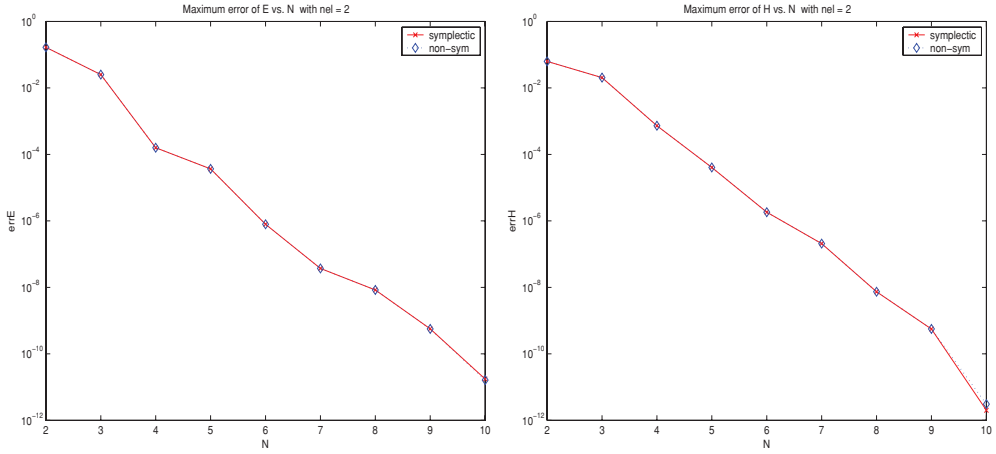

Figure 2. Errors of electric field at 2.125 T obtained by using symplectic and non-symplectic methods (left); errors of magnetic field at 2.125 T obtained by using symplectic and non-symplectic methods (right).

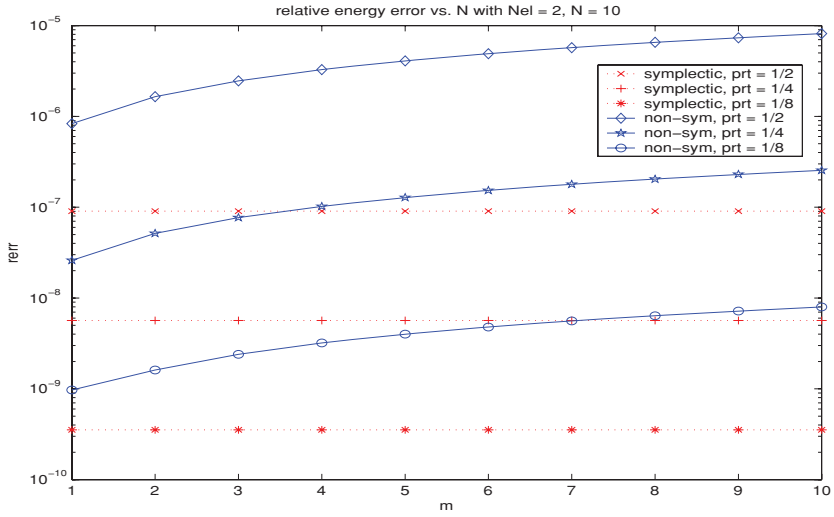

Figure 3. Errors of relative energy obtained by using symplectic and non-symplectic methods. The abscissa means that the time for termination of simulation is (100 m + 2.125) T.

method (in table 2 where $\gamma_1 = \frac{1}{2-\sqrt[3]{2}}$ and $\gamma_2 = \frac{1}{1-\sqrt[3]{4}}$) and fourth-order non-symplectic RK method (in table 3) in temporal discretization.

First, we consider a plane wave equation:

$$\begin{cases} \dfrac{\partial \mathcal{E}}{\partial t} = -c_0 \dfrac{\partial \mathcal{H}}{\partial x} \\ \dfrac{\partial \mathcal{H}}{\partial t} = -c_0 \dfrac{\partial \mathcal{E}}{\partial x}, \end{cases} \tag{24}$$

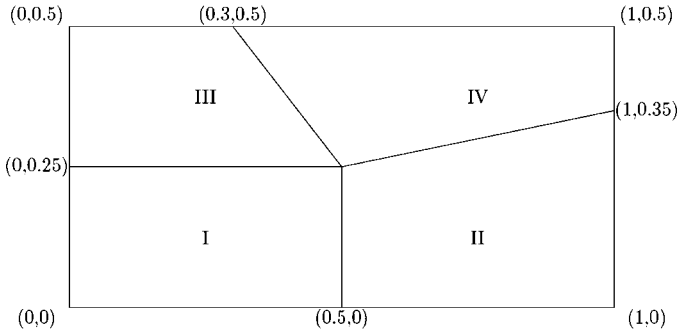

Figure 4. Domain subdivision.

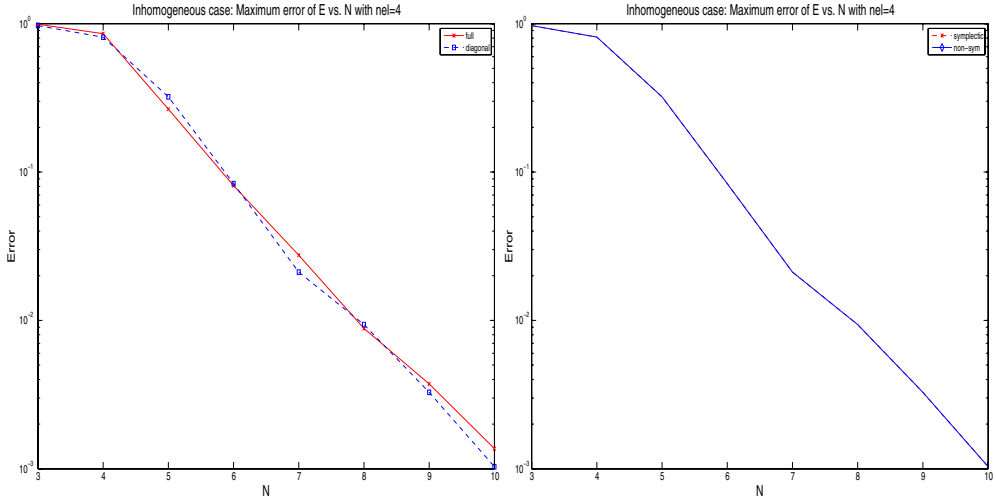

Figure 5. Errors of electric field obtained by using full and diagonal mass matrixes (left); Errors of electric field at 10T obtained by using symplectic PRK and non-symplectic RK methods (right). The elements are the four subdomains and the orders of GLL basis functions satisfy $N_\xi = N_\eta = N$.

where c_0 is the speed of light in the vacuum. The domain is [0, 0.08] and the boundary condition is $\mathcal{E} = 0$. The wavelength and the period T are equal to 0.16 ns, 0.53 ns, respectively.

As shown in figure 1, the errors of the electric (magnetic) field obtained by using full and diagonal mass matrices are very close; and in figure 2, the errors of the electric (magnetic) field obtained by using symplectic and non-symplectic methods are almost the same; in figure 3 however, the superiority of the symplectic method over non-symplectic one in preserving the energy is evident.

Next, we consider the 2D vector wave equation with the boundary condition $\mathbf{E} \times \mathbf{n} = 0$ on $\Gamma = \partial\Omega$:

$$\varepsilon \frac{\partial^2}{\partial t^2} \mathbf{E}(\mathbf{r}, t) + \frac{1}{\mu} \mathbf{curl}(\mathrm{curl}\, \mathbf{E}(\mathbf{r}, t)) = 0$$

in a rectangular cavity with dimension 1m $\times$ 0.5m as illustrated in figure 4. There are four kinds of media in the domain, their relative permittivities are 8, 4, 2, 1 in subdomains I, II, III, IV, respectively. The period is $T = 3.671$ ns and the wave number is $k_0 = 5.7095$ m^{-1}. As

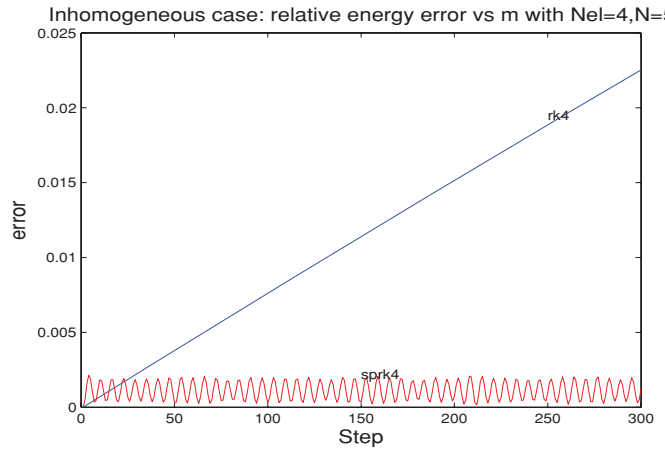

Figure 6. Errors of relative energy obtained by using symplectic PRK and non-symplectic RK methods with temporal step size 0.02 ns.

shown in figures 5 and 6, similar to the 1D case, the errors of electric field obtained by using full and diagonal mass matrices are very close; and the errors of the electric (magnetic) field obtained by using symplectic and non-symplectic methods are almost same, by the way, the spectral accuracy is influenced on account of the nonorthogonal mesh; the superiority of the symplectic method over non-symplectic one in preserving the energy is evident.

In the figures above, N, nel and prt stand for the order of the GLL basis function, the number of the elements and the temporal step size parameter, respectively.

5. Conclusions

A GLL-polynomial based SEM has been used to discretize the time-domain Maxwell's equations in spatial direction together with proper symplectic integration in temporal direction. Due to the property of GLL basis functions and symplectic methods, the proposed scheme provides high-order accuracy with little cost and preserves the structure of the obtained Poisson system. The numerical experiments have demonstrated the advantages of the SEM and the superiority of the symplectic methods over the non-symplectic ones in preserving the energies.

Acknowledgments

We would like to thank the referees for their valuable suggestions and comments that greatly helped us to improve the paper. We also thank Xiangtao Liu, Yuanchang Sun, Ningming Nie and Cangping He for helpful discussions. This research is supported by the *Informatization Construction of Knowledge Innovation* Projects of the Chinese Academy of Science '*Supercomputing Environment Construction and Application*'(INF105-SCE), and by National Natural Science Foundation of China (Grant Nos. 10471145, 10672143 and 10872037), and by Morningside Center of Mathematics, Chinese Academy of Sciences.

References

[1] Yee K S 1966 Numerical solution of initial boundary value problems involving Maxwell's equations in isotropic media *IEEE Trans. Antenna Propag.* **14** 302–7

[2] Cohen G C 2002 *High-order Numerical Methods for Transient Wave Equations* (Berlin: Springer)
[3] Jin J M 2002 *The Finite Element Method in Electromagnetics* (New York: Wiley)
[4] Monk P 1991 A mixed method for approximating Maxwell's equations *SIAM J. Numer. Anal.* **28** 1610–4
[5] Monk P 1992 Analysis of a finite element method for Maxwell's equations *SIAM J. Numer. Anal.* **29** 714–29
[6] Wong M F, Picon O and Hanna V F 1995 A finite-element method based on Whitney Forms to solve Maxwell equations in the time-domain *IEEE Trans. Magn.* **31** 1618–21
[7] Lee J F, Lee R and Cangellaris A C 1997 Time-domain finite element method *IEEE Trans. Antennas Propag.* **45** 430–424
[8] Rieben R, White D and Rodrigue G 2004 High-Order symplectic integration methods for finite element solutions to time dependent Maxwell's equations *IEEE Trans. Antennas Propag.* **52** 2190–8
[9] Lee J H and Liu Q H 2006 Analysis of 3-D eigenvalue problems based on a spectral element method *URSI Meeting Abstract* (CA: Monterey) p 30
[10] Lee J H, Xiao T and Liu Q H 2006 A 3-d spectral-element method using Mixec-order curl conforming vector basis functions for electromagnetic fields *IEEE Trans. Micro. Theor. Tech.* **54** 437–44
[11] Liu Y X, Lee J H, Xiao T and Liu Q H 2006 A spectral-element time-domain solution of Maxwell's equations *Micro. Opt Tech. Lett.* **48** 673–80
[12] Jackson J D 1999 *Classical Electrodynamics* 3rd edn (New York: Wiley)
[13] Feng K 1985 On difference schemes and symplectic geometry *Proc. 1984 Beijing Symp. on Differential Geometry and Differential Equations* (Beijing: Science Press) 42–58
[14] Sun G 1993 Construction of high order symplectic Runge-kutta methods *J. Comput. Math.* **11** 250–60
[15] Zhu W J and Qin M Z 1994 Poisson schemes for Hamiltonian systems on Poisson manifolds *Comput. Math. Appl.* **27** 7–16
[16] Lu X W and Schmid R 1997 A symplectic algorithm for wave equation *Math. Comput. Simul.* **43** 29–38
[17] Saitoh I, Suzuki Y and Takahashi N 2001 The symplectic finite difference time domain method *IEEE Trans. Magn.* **37** 3251–4
[18] Hairer E, Lubich Ch and Wanner G 2002 *Geometric Numerical Integration* (Berlin: Springer)
[19] Tang Y F, Cao J W, Liu X T and Sun Y C 2007 Symplectic methods for the Ablowitz–Ladik discrete nonlinear Schrödinger equation *J. Phys. A: Math. Theor.* **40** 2425–37
[20] Harutyunyan D 2007 Adaptive Vector Finite Element Method for the Maxwell Equations *Dissertation* University of Twente